BIOCHEMISTRY
including biophysical chemistry & molecular biology

Article

pubs.acs.org/biochemistry

Bacterial Renalase: Structure and Kinetics of an Enzyme with 2- and 6-Dihydro-β-NAD(P) Oxidase Activity from *Pseudomonas phaseolicola*

Matthew R. Hoag, Joseph Roman, Brett A. Beaupre, Nicholas R. Silvaggi, and Graham R. Moran*

Department of Chemistry and Biochemistry, University of Wisconsin−Milwaukee, 3210 North Cramer Street, Milwaukee, Wisconsin 53211-3209, United States

ABSTRACT: Despite a lack of convincing *in vitro* evidence and a number of sound refutations, it is widely accepted that renalase is an enzyme unique to animals that catalyzes the oxidative degradation of catecholamines in blood in order to lower vascular tone. Very recently, we identified isomers of β-NAD(P)H as substrates for renalase (Beaupre, B. A. et al. (2015) *Biochemistry*, *54*, 795−806). These molecules carry the hydride equivalent on the 2 or 6 position of the nicotinamide base and presumably arise in nonspecific redox reactions of nicotinamide dinucleotides. Renalase serves to rapidly oxidize these isomers to form β-NAD(P)$^+$ and then pass the electrons to dioxygen, forming H_2O_2. We have also shown that these substrate molecules are highly inhibitory to dehydrogenase enzymes and thus have proposed an intracellular metabolic role for this enzyme. Here, we identify a renalase from an organism without a circulatory system. This bacterial form of renalase has the same substrate specificity profile as that of human renalase but, in terms of binding constant (K_d), shows a marked preference for substrates derived from β-NAD$^+$. 2-dihydroNAD(P) substrates reduce the enzyme with rate constants (k_{red}) that greatly exceed those for 6-dihydroNAD(P) substrates. Taken together, k_{red}/K_d values indicate a minimum 20-fold preference for 2DHNAD. We also offer the first structures of a renalase in complex with catalytically relevant ligands β-NAD$^+$ and β-NADH (the latter being an analogue of the substrate(s)). These structures show potential electrostatic repulsion interactions with the product and a unique binding orientation for the substrate nicotinamide base that is consistent with the identified activity.

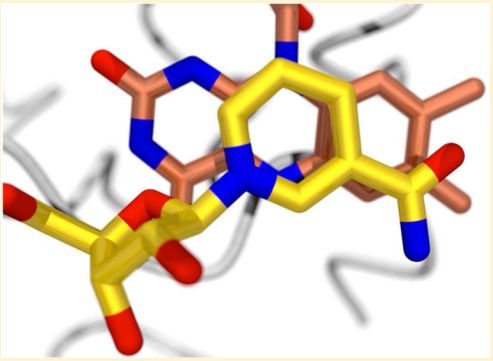

Renalase (EC 1.6.3.5) was discovered in 2005 and purported to be a flavoprotein hormone produced by the kidney that catalyzes the oxidation of catecholamines in order to lower blood pressure and slow the heart.[1,2] However, the initial experiments used to identify the substrates focused on only a handful of molecules and did not include control reactions to account for the inexorable oxidation of catecholamines in oxygenated buffer. Despite claimed physiological verifications of this activity,[2−7] no convincing *in vitro* evidence of catecholamine oxidase activity has been offered. The deficiencies in the original methods were compounded in subsequent claims that suggested an, as isolated, quiescent renalase state and ever more unlikely chemistries for which catalysis and the stoichiometry were not established.[8,9] A number of researchers have attempted to counter the expanding belief that renalase catalysis is associated with vascular tone, by either questioning the original methods used to establish activity[10,11] or demonstrating that, relative to appropriate controls, there is no evidence of catecholamine consumption by the enzyme.[12] These refutations have gone largely unheeded, and the preponderance of scientific studies pertaining to renalase continue to be predicated on passive acceptance of an unproven catalytic role.[2−8,13−38]

We have recently shown that human renalase (HsRen) is indeed a flavoprotein oxidase, but it is one that catalyzes the oxidation of β-NAD(P)H isomers. These isomers carry the hydride on the nicotinamide base in the noncanonical 2 and 6 positions (2- and 6-dihydroNAD(P)) (Scheme 1). The oxidation of these isomers occurs as much as 5 orders of magnitude more rapidly than any prior claim for renalase activity, and the turnover reaction with these molecules has a defined stoichiometry and substrate specificity profile. Moreover, we have proposed that the purpose of this activity is to avoid inhibition of primary metabolism by these NAD(P)H isomers that have low nanomolar K_i values for specific dehydrogenases.[39−41] If 2- and 6-dihydroNAD(P) molecules are prone to form in nonenzymatic reduction reactions of β-NAD(P)$^+$ and are truly a detriment to respiratory activity, then it is reasonable to assume that this is an intracellular enzymatic activity that will exist in organisms that do not have a circulatory system.

The structure of HsRen was determined by the Aliverti group in 2011[42] using the model of a generically assigned amine oxidase from *Pseudomonas syringae* (PDB ID 3KKJ) whose structure was solved and deposited in the Protein Data Bank (PDB) by the North East Structural Genomics Consortium (NESGC). While not homologous with the HsRen primary structure (19.5% identitical), this protein had

Received: April 24, 2015
Revised: May 25, 2015
Published: May 27, 2015

DOI: 10.1021/acs.biochem.5b00451
Biochemistry 2015, 54, 3791−3802

Scheme 1. Observed Activities of Renalase

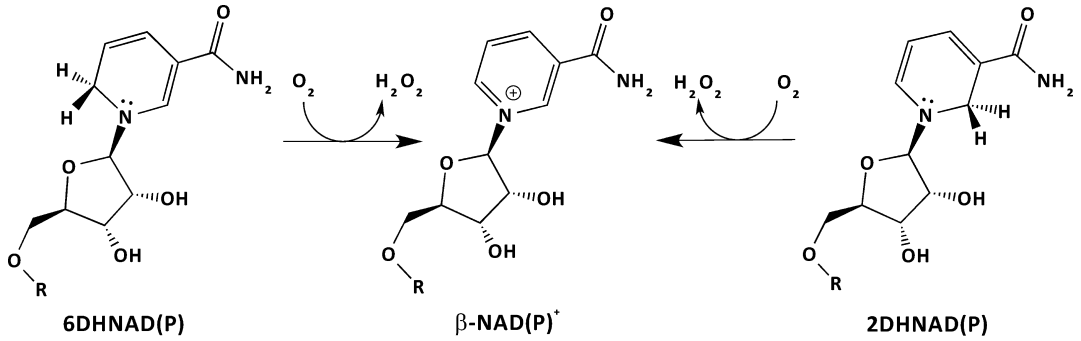

the renalase fold (a topology that is common to numerous redox-active flavoproteins[43−48]) and a very similar constellation of active site residues proximal to the FAD isoalloxazine.[42] We surmised that this protein was likely a bacterial form of renalase. In this article, we show that this amine oxidase from *P. syringae* (van Hall pathovar *phaseolicola* strain 1448A) harbors the same catalytic activity as that observed for HsRen but with unique kinetic properties and stark substrate preferences. We also present the X-ray crystal structures of this enzyme in complex with nicotinamide dinucleotides that show a reductive pose of the nicotinamide base with respect to the flavin cofactor that is consistent with the proposed activity.

MATERIALS AND METHODS

Materials. β-NAD$^+$ was sourced from Sigma-Aldrich. Sodium borohydride, potassium phosphate (mono and dibasic), sodium formate, and glycerol were from Acros. Sep-Pak C18 (35 cc) cartridges were purchased from Waters. Competent NEB5α and BL21 DE3 *Escherichia coli* cells were obtained from New England Biolabs. Talon metal affinity resin was from Thermo-Fisher Scientific. Sodium acetate was purchased from Mallinckrodt. 2- and 6-DHNAD and 2- and 6-DHNADP were prepared using an adaptation of our previously published methods.[39] Both sets of substrates were formed by sodium borohydride reduction of β-NAD$^+$ or β-NADP$^+$. The products of reduction, β-NAD(P)H, 2-dihydroNAD(P) (2DHNAD(P), and 6-dihydroNAD(P) (6DHNAD) (and residual β-NAD(P)+) were separated using a Waters X-Bridge 19 × 250 mm, 5 μM C18 column. 6DHNAD(P) molecules were relatively stable and could be prepared as previously described and stored indefinitely at −80 °C, whereas 2DHNAD(P) molecules were unstable and used immediately after collection from preparative HPLC.

Spectrophotometric Quantification. Dihydronicotinamide chromophore extinction coefficients were as follows: β-NADH, β-NADPH: $\varepsilon_{340\ nm}$ = 6220 M^{-1} cm^{-1};[49] 2DHNAD(P): $\varepsilon_{394\ nm}$ = 5360 M^{-1} cm^{-1}; 6DHNAD(P): $\varepsilon_{345\ nm}$ = 6580 M^{-1} cm^{-1}; and β-NAD$^+$: $\varepsilon_{260\ nm}$ = 18 800 M^{-1} cm^{-1}.[39] *P. syringae* renalase (PpRen) was quantified using the measured extinction coefficient for the enzyme-bound flavin ($\varepsilon_{452\ nm}$ = 11 000 M^{-1} cm^{-1}), determined using an SDS denaturation method as previously described.[50]

Expression and Purification of PpRen. A plasmid derived from pET21a (pET21_NESG) containing the gene for PpRen was provided by the NESGC. This construct was prepared by PCR amplification of the PpRen gene from *P. syringae* (van Hall pathovar *phaseolicola* strain 1448A) followed by cloning into NdeI and XhoI restriction sites and fusing the PpRen gene to a C-terminal 6×His-tag. This construct has a single variant amino acid from what is reported for this *phaseolicola* strain: a serine is coded in place of glycine 145. The plasmid was transformed into competent BL21 DE3 cells, plated onto Luria−Bertani (LB) agar (100 μg/mL ampicillin), and grown overnight at 37 °C. Individual colonies were then selected and grown in LB broth with shaking (250 rpm) at 37 °C until growth reached early log phase. One milliliter of cell stocks was made by adding filter-sterilized glycerol to a final concentration of 20% and then storing at −80 °C.

For expression, 1 mL cell stocks were thawed, plated onto LB agar containing 100 μg/mL ampicillin, and grown overnight at 37 °C (100 μL cells/plate). The lawn of cells obtained was resuspended in LB broth and transferred to LB broth cultures (two plates/L of broth) and grown at 37 °C in a shaking incubator (220 rpm) until mid log phase (OD_{600nm} = 0.8). The temperature was then decreased to 17 °C, and the culture was grown to OD_{600nm} ∼ 1.0 (∼1−2 h) and induced with 0.1 mM IPTG. Thirty hours after induction, the cells were harvested by centrifugation (4000*g* for 30 min) and subjected to one freeze/thaw cycle. All purification steps were performed at 4 °C. Cell pellets were resuspended in 20 mM sodium HEPES buffer, pH 7.5 (approximately 20 mL/L culture), placed in a stainless steel beaker, and lysed by sonication using a Branson 450 sonicator (3 × 240 s at 50 W). During this procedure, the cell suspension vessel was seated in a slurry of ice and water. Lysed cells were centrifuged at 12 800*g* for 30 min, the pellet was discarded, and the supernatant was loaded onto a 12.5 × 150 mm Co^{2+} Talon affinity column equilibrated with 20 mM sodium HEPES buffer, pH 7.5. Initially contaminating proteins were eluted with 200 mL of 10 mM imidazole, 20 mM sodium HEPES buffer adjusted to pH 7.5 with H_2SO_4; then, a gradient from 10 to 300 mM imidazole in the same buffer was used to elute ostensibly pure PpRen as a single symmetrical peak. Distinctly yellow fractions were pooled. Imidazole was removed, and the buffer was exchanged to 10 mM potassium phosphate, pH 7.5, by dialysis using 10 kDa nominal molecular weight cutoff dialysis tubing to achieve a net ≥100 000-fold buffer exchange. Aliquots of purified concentrated renalase (<120 μM) were then stored at −80 °C.

Analytical HPLC. Evidence of the substrate specificity profile was obtained by adding sodium borohydride (250 μM) to β-NAD(P)$^+$ (250 μM). The sample was divided into two, and PpRen (30 μM) was added to one and incubated for 3 min, whereas the other was frozen in liquid nitrogen. PpRen was then removed from the first sample by centrifugal ultrafiltration using a 0.5 mL Amicon 10 kDa cutoff filter. Both samples were then chromatographed by analytical HPLC. Separation of the resulting mixtures was achieved using a Waters X-Bridge 4.6 × 150 mm, 3.5 μM C18 column coupled to a Waters 600E pump

DOI: 10.1021/acs.biochem.5b00451
Biochemistry 2015, 54, 3791−3802

Scheme 2. Model for the Reductive Half-Reaction

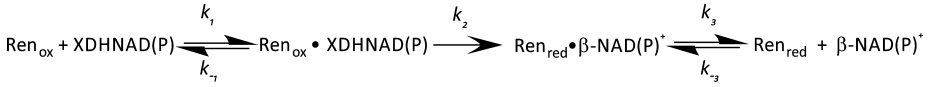

and Waters 2487 dual-wavelength detector. Elution of components of the mixture was observed simultaneously at 260 and 340 (or 394) nm. The components were separated isocratically at 1.0 mL/min in either 10 mM (β-NAD$^+$ derived) or 50 mM (β-NADP$^+$ derived) potassium phosphate buffer, pH 7.5.

Reductive Half-Reaction of PpRen with 6DHNAD(P). The reductive half-reaction of PpRen could be observed independent of subsequent oxidative processes by exclusion of dioxygen using previously published methods.[51] Anaerobic PpRen (5 mL, 14−16 μM) in 20 mM potassium phosphate buffer containing 1 mM dextrose and 5 U/mL glucose oxidase (25 μL, 25 units) was mounted onto a Hitech (now TgK) DX2 stopped-flow instrument that had been scrubbed of residual dioxygen by incubation for 16 h with a solution of 1 mM dextrose, 10 U/mL glucose oxidase. 6DHNAD(P) samples were thawed and diluted to target concentrations in water containing 1 mM glucose. 2DHNAD(P) was collected into a glass syringe (that had a small amount of concentrated dextrose added prior (≤1 mM final)) directly from preparative HPLC, diluted to approximate target concentration, and used immediately. All substrate solutions were sparged with argon gas for 5 min. Before capturing and mounting the substrate solution to the stopped-flow instrument, 10 μL of glucose oxidase (10 units) was injected via the luer tip.

Anaerobic PpRen and substrate solutions were mixed, and reduction of the renalase cofactor was observed at the absorption maximum of PpRen FAD, 452 nm. The stability of the 6DHNAD substrate allowed for it to be prepared in sufficient quantity to achieve a high range of concentrations, ranging from second- to pseudo-first-order reaction conditions. The pseudo-first-order data were fit to a linear combination of two exponentials according to eq 1 using Kinetic Studio software (TgK Ltd.). In this equation, A_1 and A_2 are the amplitudes associated with the first and second rate constants, $k_{1,obs}$ and k_2, respectively, and C is the absorbance at end of the reaction. The dependence of the observed rate constants ($k_{1,obs}$) for the largest amplitude phase (~90%) was fit to the hyperbolic form of the single-site binding equation (eq 2) according to Strickland, where k_{red} is the limiting rate constant for reduction and $K_{6DHNAD(P)}$ is the binding constant for 6DHNAD.[52] 2DHNAD(P) is prone to decompose within minutes. Reduction data for these substrates were obtained primarily from second-order reactant ratios and as such could not be fit meaningfully to linear combinations of exponential terms. The data for 2DHNAD(P) substrates were fit to a the mechanism depicted in Scheme 2 using KinTek Explorer to obtain the dissociation constant for the substrate (k_{-1}/k_1) and the intrinsic rate constant for reduction (k_2). The concentration of these substrates was estimated by recording a spectrum immediately prior to and immediately after each kinetic observation and averaging.

$$A_{452nm} = A_1(e^{-k_{1,obs}t}) + A_2(e^{-k_2t}) + C \quad (1)$$

$$k_{obs} = \frac{k_{red}[6DHNAD(P)]}{(K_{6DHNAD(P)} + [6DHNAD(P)])} \quad (2)$$

Oxidative Half-Reaction of PpRen. Reoxidation of the renalase cofactor in the presence of dissolved dioxygen was observed by double-mixing stopped-flow spectrophotometry. PpRen (16 μM) was prepared in a tonometer in an equivalent manner to that of the reductive half-reaction (though without dextrose or glucose oxidase). In the first mix, this solution was combined with 12 μM 6DHNAD. The reduction reaction was allowed to proceed for 150 s prior to the second mix that introduced dissolved dioxygen of defined concentration (final concentrations after the second mix were 4 μM PpRen, 3 μM β-NAD$^+$, varied dioxygen). The dissolved oxygen concentration in this solution was defined by sparging an inverted syringe containing 10 mM phosphate buffer, pH 7.5, with blended dinitrogen and dioxygen gases of known partial pressures supplied by a Maxtec Maxblend gas blender. The concentration of dissolved oxygen was confirmed by first sparging the reaction chamber of a Hansatech dioxygen electrode filled with the same buffer to define the equilibrium concentration of dissolved dioxygen. The reduced anaerobic PpRen solution was then mixed and the ensuing reoxidation observed at 452 nm. The data were fit to eq 3, in which $k_{ox,obs}$ is the observed rate constant for reoxidation, A_1 is the absorption amplitude for the phase observed, and C is the end point absorbance. The dependence of the observed rate constant was fit to a straight line that passed through the origin according to eq 4, where k_{ox} is the second-order rate constant for reoxidation and $[O_2]$ is the concentration of dioxygen.

$$A_{452nm} = A_1(e^{-k_{ox,obs}t}) + C \quad (3)$$

$$k_{ox,obs} = k_{ox}[O_2] \quad (4)$$

The influence of β-NAD$^+$ on the rate constant for reoxidation was observed by similar methods as those described above using the double-mixing facility of the stopped-flow instrument. PpRen (23.2 μM) was mixed with 6DHNAD (20 μM) and allowed to age for 150 s. This mixture was then mixed with 238 μM dioxygen, and the reoxidation was observed at 452 nm. β-NAD$^+$ (0−4 mM) was then added to the third solution, and the experiment was repeated. The dependence of the observed rate constant for reoxidation ($k_{ox,obs}$) was then fit to eq 5 to determine the extent of inhibition (Δk_{ox}) and the binding constant for β-NAD$^+$ to the reduced form of the enzyme (K_{NAD^+}), where k^i_{ox} is the rate constant observed in the absence of exogenous β-NAD$^+$.

$$k_{ox,obs} = k^i_{ox} - \left(\frac{\Delta k_{ox}[NAD^+]}{K_{NAD^+} + [NAD^+]}\right) \quad (5)$$

Dissociation Constants for the PpRen$_{ox}$·β-NADH, PpRen$_{ox}$·β-NADPH, and PpRen·SO$_3$ Adduct Complexes. The dissociation constants for the PpRen$_{ox}$·β-NADH, PpRen$_{ox}$·β-NADPH, and PpRen·SO$_3$ complexes were measured by perturbation of the renalase flavin spectrum when each ligand was titrated. For both the β-NADH and β-NADPH titrations, slow noncatalytic reduction of the PpRen flavin during the experiment (0.0008 s^{-1}) was avoided by preparing 11 stocks of 0.9 mL (17 μM for β-NADH, 12 μM for β-NADPH) of the

DOI: 10.1021/acs.biochem.5b00451
Biochemistry 2015, 54, 3791−3802

enzyme in 10 mM potassium phosphate buffer, pH 7.5, at 25 °C. To each 0.9 mL aliquot was added 0.1 mL of a range of β-NADH or β-NADPH stocks, and the spectrum was recorded. As such, the spectrophotometric data are compiled from 11 PpRen renalase samples after the addition of β-NADH (0−1 mM) or β-NADPH (0−7 mM).

Titration of PpRen with sodium sulfite formed a labile sulfite adduct that is commonly observed with flavoprotein oxidases. In this experiment, 7 μM PpRen in 10 mM potassium phosphate buffer, pH 7.5 (25 °C), was titrated with sulfite by incremental additions spanning the range 0−310 mM. Spectra were recorded after each addition.

For β-NADH and sufite titrations, spectra were recorded using a Shimadzu 1800 UV−vis spectrophotometer. For the β-NADPH titration, spectra were recorded using a Shimadzu 2600 UV−vis spectrophotometer. After correction for dilution, the changes in absorption at 492, 468, and 452 nm were used to determine the dissociation constants for the Ren_{ox}·β-NADH, Ren_{ox}·β-NADPH, and the Ren_{ox}·β-NAD^+ complexes, respectively. The changes in absorption were fit to the quadratic solution form of the single site binding equation (eq 6) in which [E] is the PpRen concentration, [EL] is the concentration of the PpRen·ligand complex, and K_L is the dissociation constant of the PpRen·ligand complex. For β-NADH, β-NADPH, and sulfite, the raw data were fit. That is, the change in absorbance at defined wavelengths was used as a measure of [EL], and the maximal change in absorbance, as a representation of [E].

$$[EL] = (([L] + [E] + K_L) - \sqrt{([L] + [E] + K_L)^2 - 4([L] + [E])})/2 \quad (6)$$

Crystallization, Structure Determination, and Model Refinement. Initial crystallization conditions were those identified by the NESGC and included 2 M sodium formate, 100 mM sodium acetate, pH 4.6, at 20 °C. Diffraction-quality crystals were obtained by the hanging-drop vapor diffusion method. The droplet was formed from three 1 μL additions: 1 μL of the well solution, 1 μL of PpRen (104 μM), and 1 μL of H_2O. Crystals appeared after 2−4 days and grew to maximal dimensions of ∼200 × 50 × 10 μm^3. Crystals were harvested from the hanging drops and soaked for 1−3 min in 2.5 M sodium formate, 120 mM sodium acetate, pH 4.7, with 20% glycerol and 166 mM β-NAD^+ or 10 mM β-NADH. The mounted crystal was then flashed-cooled in liquid nitrogen. Crystals were initially screened for diffraction quality using the rotating anode X-ray source at Marquette University (Milwaukee, WI). X-ray diffraction data for PpRen·β-NAD^+ were collected at beamline 21-ID-D of the Life Science Collaborative Access Team (LS-CAT) at the Advanced Photon Source (APS). Data for the PpRen·β-NADH complex were collected at LS-CAT beamline 21-ID-F. Data were processed with HKL2000.[53]

The structure of PpRen was determined by molecular replacement in PHASER[54] with a search model derived from chain A of the *P. syringae* Q888A4 renalase structure (PDB ID 3KKJ, Northeast Structural Genomics Consortium) with all nonprotein atoms removed and all B-factors set to 20.0. After iterative cycles of manual model building in COOT[55] and maximum likelihood based refinement using the PHENIX package (phenix.refine),[56] ordered solvent molecules were added in phenix.refine automatically and culled manually in COOT. After adding solvent atoms, the FAD cofactor and β-NAD^+ or β-NADH were added to the model in COOT. During the last rounds of refinement, hydrogen atoms were added to the model using phenix.reduce[57] to improve the stereochemistry of the model. Positions of H atoms were refined using the riding model with a global B-factor. Regions of each model to be used in translation-libration-screw (TLS) refinement were identified using phenix.find_tls_groups, and the TLS parameters were refined in phenix.refine. Once the refinement converged, the model was validated using the tools implemented in COOT and PHENIX.[58,59] Side chains with poor or missing electron density were modeled in favored rotameric conformations. The B-factors were allowed to refine without additional restraints, and the occupancies were held to 1.0. Data collection and model refinement statistics are listed in Table 1. Coordinates and structure factors for the PpRen·β-NAD^+ and PpRen·β-NADH complexes have been deposited in the Protein Data Bank with accession codes 4ZCD and 4ZCC, respectively.

RESULTS

Properties of PpRen and Substrate Identification. PpRen can be expressed by the above methods to yield ∼17 mg of purified enzyme per liter of culture. The absorption spectrum of the purified enzyme indicates characteristic visible maxima

Table 1. Crystallographic Data Collection and Model Refinement Statistics

	PpRen·β-NAD^+	PpRen·β-NADH
space group	*C*2	$P2_1$
unit cell parameters	*a* = 144.7, *b* = 37.6, *c* = 138.2 Å, α = γ = 90, β = 120°	*a* = 63.5, *b* = 71.5, *c* = 143.8 Å, α = γ = 90, β = 97.5°
resolution (Å) (last shell)	33.2−1.66 (1.69−1.66)	46.2−2.00 (2.03−2.00)
wavelength (Å)	0.97895	0.97872
no. of reflections		
observed	286 455 (12 871)	328 721 (15 867)
unique	76 829 (3588)	86 594 (4305)
completeness (%)[a]	99.7 (94.0)	100.0 (100.0)
R_{merge} (%)[a,b]	0.044 (0.336)	0.096 (0.628)
multiplicity	3.7 (3.6)	3.8 (3.7)
$\langle I/\sigma(I)\rangle$[a]	26.3 (3.7)	13.7 (2.2)
model refinement statistics		
reflections in work set	73 035	77 722
reflections in test set	2971	2892
R_{cryst} (R_{free})	0.151 (0.176)	0.170 (0.215)
no. of residues	651	1288
no. of solvent atoms	748	736
number of tls groups	4	28
Average B-Factor (Å²)[c]		
protein atoms	16.0	33.1
ligand atoms	15.5	32.5
solvent	28.8	36.6
RMS Deviations		
bond lengths (Å)	0.012	0.014
bond angles (deg)	1.490	1.634
coordinate error (Å)	0.15	0.19

[a]Values in parentheses apply to the high-resolution shell indicated in the resolution row. [b]$R = \sum(||F_o| - \text{scale} \times |F_c||)/\sum |F_o|$. [c]Isotropic equivalent B-factors, including contribution from TLS refinement.

DOI: 10.1021/acs.biochem.5b00451
Biochemistry 2015, 54, 3791−3802

indicative of bound flavin. The flavin maxima are observed at 380 nm (ε = 10.1 mM^{-1} cm^{-1}) and 452 nm (ε = 11 mM^{-1} cm^{-1}), distinct from those observed for HsRen (385 nm (ε = mM^{-1} cm^{-1}), 458 nm (ε = 11.3 mM^{-1} cm^{-1})) and free flavin (375 nm (ε = 9.7 mM^{-1} cm^{-1}), 450 nm (ε = 11.3 mM^{-1} cm^{-1})). The enzyme is stable at 25 °C and below in phosphate buffer at pH 7.5, but it is prone to precipitate at concentrations above 4.5 mg/mL (~120 μM).

Borohydride reduction of β-NAD^+ or β-$NADP^+$ yields three reduced isomers of each: 2-dihydroNAD(P) (2DHNAD(P)), 4-dihydroNAD(P) (β-NAD(P)H), and 6-dihydroNAD(P) (6DHNAD(P)). We have shown that HsRen catalytically oxidizes both 2- and 6DHNAD(P) to form β-$NAD(P)^+$.[39] HPLC analysis indicated that when PpRen was added to the mixture of reduction products only 2- and 6DHNAD(P) molecules were consumed (Figure 1), indicating that this

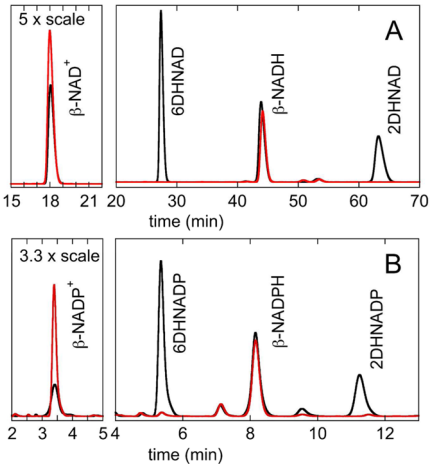

Figure 1. Analytical HPLC of renalase turnover reactions of borohydride reduced mixtures of β-NAD(P)H isomers. HPLC separation was achieved using an analytical Waters X-bridge C18 column run isocratically in potassium phosphate buffer (10 mM for NAD derived mixtures and 50 mM for NADP derived mixtures). All eluting species were detected at 260 nm, the absorption maximum for the NAD(P) adenine base. (A) The black chromatogram is the separation of the components formed from borohydride reduction of β-NAD^+. The red chromatogram is 3 min after the addition of 30 μM PpRen. (B) The black chromatogram is the separation of the components formed from borohydride reduction of β-$NADP^+$. The red chromatogram is 3 min after the addition of 30 μM PpRen.

Pseudomonas form of renalase has the same substrate profile as that of the human form. When chromatographed at 260 nm, where the adenine chromophore has maximal absorption, the net concentration lost from the 2- and 6DHNADP peaks (based on standard curves for each) was gained by the β-$NAD(P)^+$ peak, indicating that the product formed from both types of substrate is the oxidized form of the nicotinamide dinucleotide (Scheme 1).

Reductive Half-Reaction of PpRen with 6DHNAD(P). The reductive half-reaction was observed by mixing PpRen with varied concentrations of 6DHNAD, 6DHNADP, 2DHNAD, and 2DHNADP in the absence of molecular oxygen. The transfer of a hydride from the DHNAD(P) substrate to the PpRen flavin is observed as a large change in extinction coefficient of the flavin as it converts to the reduced state (Figure 2). The equilibrium and kinetic constants derived from these experiments are summarized in Table 2. Both 6DHNAD and 6DHNADP were titrated, and the largely monophasic reduction and hyperbolic dependence of the observed rate constant for reduction indicated that these substrates bind rapidly and reversibly to the enzyme prior to hydride transfer. The substrate dissociation constants obtained from the reductive-half reaction data indicated relative higher binding affinity for β-NAD^+-derived substrates (K_{2DHNAD} ~ 36 μM, K_{6DHNAD} ~ 28 μM) compared to that for β-$NADP^+$-derived substrates ($K_{2DHNADP}$ ~ 500 μM, $K_{6DHNADP}$ ~ 1400 μM). This apparent preference for β-NAD^+-derived substrates is consistent with our proposed function for renalase: to protect primary metabolism dehydrogenases from inhibition by 2- and 6DHNAD.[39] However, both 6-dihydro substrates exhibited a relative slow reduction rate constant ($k_{red,6DHNAD}$ = 0.4 s^{-1}, $k_{red,6DHNAP}$ = 0.5 s^{-1}), approaching 3 orders of magnitude slower than those observed for the 2-dihydro forms ($k_{red,2DHNAD}$ ~ 180 s^{-1}, $k_{red,2DHNAP}$ ~ 120 s^{-1}). When these data are viewed as a ratio, they define a measure of substrate capture (k_{red}/K_d); it is apparent that PpRen has a 20-fold preference for 2DHNAD over its next preferred substrate, 2DHNADP (Table 2). Both β-NAD^+- and β-$NADP^+$-derived substrates accelerate the reduction rate constant by 10^3 to 10^5 compared to that observed for β-NADH (~0.0008 s^{-1} at 2 mM β-NADH). A pronounced preference for the position of the nicotinamide hydride was not observed for HsRen that exhibited ostensibly the same dissociation constant for either β-NAD^+-derived substrate isomers (K_{2DHNAD}, K_{6DHNAD} ~ 170 μM) and only modest differences in the reduction rate constant ($k_{red,6DHNAD}$ ~ 230 s^{-1}, $k_{red,2DHNAP}$ ~ 850 s^{-1}).[39]

Oxidative Half-Reaction of PpRen. The reoxidation of PpRen was observed by double-mixing stopped flow. The anaerobic oxidized enzyme was first mixed with anaerobic 6DHNAD at a concentration sufficient to reduce 75% of the enzyme. After a 150 s age time that accounted for >6 half-lives for the predicted reduction rate constant at the reactant concentrations used, the partially reduced enzyme was mixed with defined pseudo-first-order concentrations of dioxygen and observed to reoxidize at 452 nm (Figure 3A). The dependence of the observed reoxidation rate constant on the concentration of dioxygen was linear with a zero intercept, indicating a collision-based reaction (Figure 3A inset). The second-order reoxidation rate constant was obtained from the slope of the dependence according to eq 4 and was found to be 5 × 10^3 M^{-1} s^{-1}, similar to that observed for HsRen (2.9 × 10^3 M^{-1} s^{-1}).[51]

Exogenous β-NAD^+ impeded the rate constant for reoxidation (Figure 3B). The dependence of the inhibition yielded a dissociation constant for the PpRen(red)·β-NAD^+ complex of 230 μM (Figure 3B, inset), 7-fold higher affinity than that of the same complex in HsRen. Suppression of the reoxidation rate constant extrapolated to ~0 s^{-1}, indicating an ordered product release mechanism in which β-NAD^+ (and presumably β-$NADP^+$) must dissociate before dioxygen can react with the reduced flavin cofactor. This differs from HsRen, whose reoxidation rate constant was not influenced by exogenous nicotinamide product and as such displayed a formally random product release mechanism.[51]

Dissociation Constants for the $PpRen_{ox}$·β-NADH, $PpRen_{ox}$·β-NADPH, and PpRen·SO_3 Adduct Complexes. The dissociation constants for β-NADH and β-NADPH were measured by titration and observation of the changes in the absorption spectrum of the PpRen FAD isoalloxazine moiety (Figure 4A). Consistent with the apparent preference for β-

DOI: 10.1021/acs.biochem.5b00451
Biochemistry 2015, 54, 3791−3802

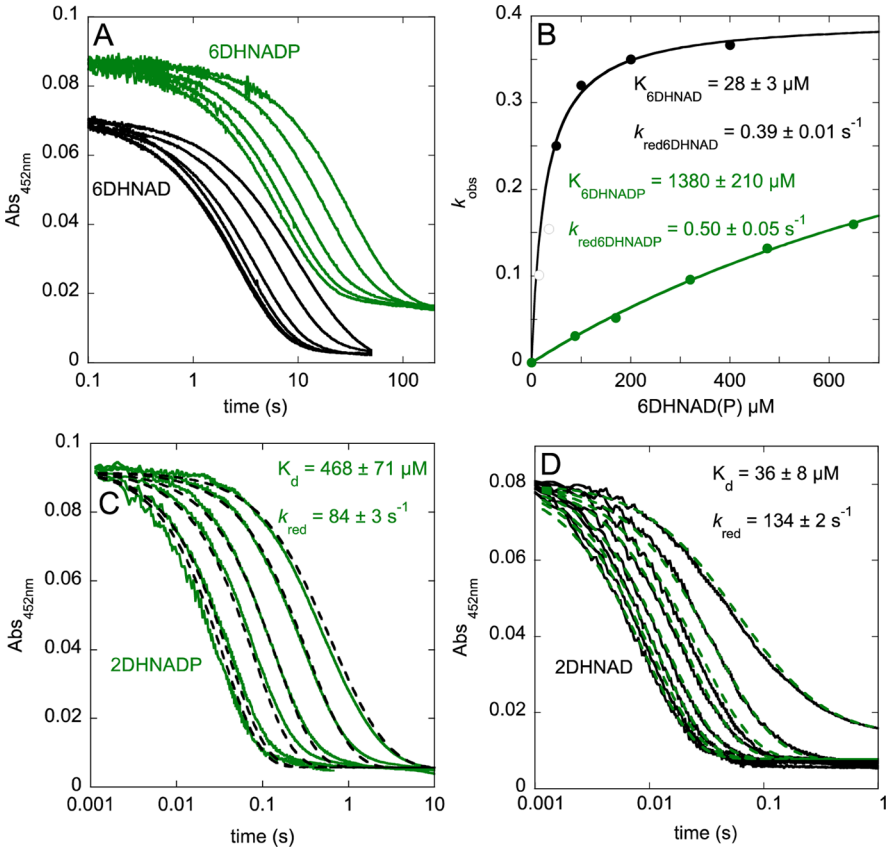

Figure 2. Kinetics of the reductive half-reactions of PpRen with nicotinamide dinucletide substrates. Oxidized anaerobic PpRen was mixed with varied concentrations of anaerobic substrates, and the reduction of the enzyme's cofactor was observed at 452 nm. (A) Reduction of the PpRen by 6DHNAD(P) substrates. Approximately 7 μM PpRen was reacted with either 6DHNAD (15, 35, 50, 100, 200, 400 μM) or 6DHNADP (88, 170, 320, 475, 613 μM). Traces for 6DHNAD are offset (down) for clarity. (B) The dependence of the observed rate constant for reduction on the concentration of 6DHNAD and 6DHNADP fit to the hyperbolic form of the single site binding equation (eq 2). NB: observed rate constants obtained from exponential fits to non-pseudo-first-order reactant concentrations for 6DHNAD are shown as open circles. (C) The reduction of PpRen (8 μM) by 2DHNADP (11.3, 21.5, 49.8, 93.0, 211.9, 263.8 μM) fit globally (dashed lines) to the model shown in Scheme 2. (D) The reduction of PpRen (8 μM) by 2DHNAD (6.3, 13.0, 19.0, 26.4, 45.6, 72.1, 97.2, 163.2 μM) fit globally (dashed lines) to the model shown in Scheme 2. For (C) and (D), concentrations are based on the average of two spectra: one recorded immediately prior to and one immediately after collection of kinetic data.

Table 2. Summary of Kinetic and Equilibrium Constants for PpRen

substrate/ligand	K_d (μM)	k_{red} (s^{-1})	k_{red}/K_d (μM^{-1} s^{-1})
2DHNAD	36 ± 8	134 ± 2	3.7 ± 0.8
2DHNADP	468 ± 71	84 ± 3	0.18 ± 0.02
6DHNAD	28 ± 3	0.39 ± 0.01	0.014 ± 0.002
6DHNADP	1380 ± 210	0.50 ± 0.05	$3.6 \pm 0.7 \times 10^{-4}$
β-NADH	81 ± 7	~0.000080 ± 0.000001	$9.8 \pm 0.8 \times 10^{-6}$
β-NADPH	1540 ± 370	[a]	

[a]Not measured.

NAD^+-derived substrates, the dissociation constant for the PpRen·β-NADH complex was found to be ~80 μM, comparable to that for the 2DHNAD and 6DHNAD substrates (Figure 4). This low level of β-NADH isomer selectivity was also observed in the human enzyme[39] and indicates that renalases are not able to discriminate between each of the reduced forms of β-NADH and therefore function in a partially inhibitory ligand environment. However, the PpRen·β-NADH dissociation constant is 7-fold lower than that measured for the human enzyme, facilitating soaking strategies intended to form this complex in the crystal state (*vide infra*). Consistent with the dissociation constants measured in the reductive half-reaction for 6DHNADP and 2DHNADP, the dissociation constant for β-NADPH was observed to be 19-fold larger than that for β-NADH.

Flavin−sulfite adduct formation is a peculiar characteristic of many oxidase enzymes. The Aliverti group showed that natively folded HsRen formed a dissociable sulfite adduct with the flavin cofactor.[42] In order to offer an additional reactivity correlation to HsRen, we titrated sulfite to PpRen (Figure 4B). Characteristic bleaching of the long-wavelength transitions of the flavin spectrum were observed along with the appearance of a UV transition at ~320 nm. When the data obtained at 452 nm were fit to the quadratic solution of the single-site binding

DOI: 10.1021/acs.biochem.5b00451
Biochemistry 2015, 54, 3791−3802

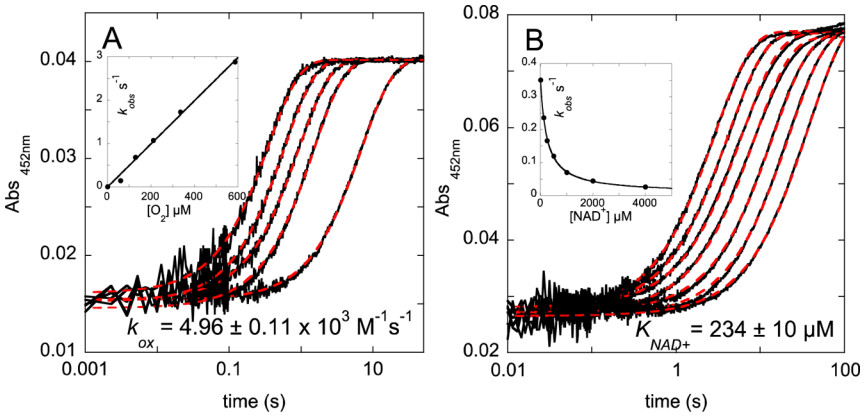

Figure 3. Kinetics of the oxidative half-reaction of PpRen. (A) Reoxidation of PpRen in the presence of varied concentrations of molecular oxygen observed at 452 nm. Reduced anaerobic PpRen (3 μM) was reacted with pseudo-first-order concentrations (59, 128, 210, 335, 587 μM) of dioxygen. Traces were fit to eq 3 (red dashes). Inset: The dependence of the observed rate constant for reoxidation on the concentration of added β-NAD$^+$. Traces are shown for 5.8 μM PpRen reoxidizing in the presence of 119 μM dioxygen with 0, 125, 250, 500, 1000, 2000, or 4000 μM added β-NAD$^+$ fit to eq 3 (red dashes). Inset: The dependence of the observed rate constant for reoxidation on the concentration of exogenous β-NAD$^+$ fit to eq 5.

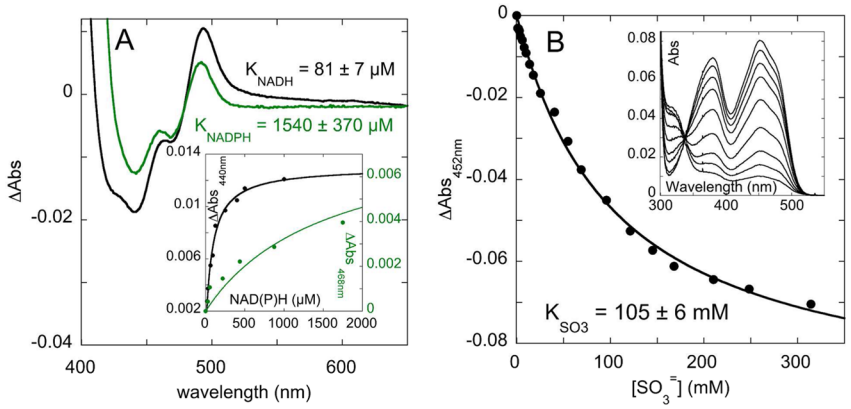

Figure 4. Measurement of the dissociation constants for the PpRen$_{ox}$·β-NADH, PpRen$_{ox}$·β-NADPH, and PpRen·SO$_3$ complexes. (A) Flavin difference spectra and binding isotherms for the association of NADH and NADPH with PpRen. For the PpRen$_{ox}$·β-NADH titration (black), 17 μM PpRen was titrated with NADH (0−1 mM) and the spectrum at each ligand concentration was recorded. The observed absorption changes in the spectrum at 494 nm were fit to eq 5 (inset). For the PpRen$_{ox}$·β-NADPH titration (green), 12 μM PpRen was titrated with NADPH (0−7 mM) and the spectrum at each ligand concentration was recorded. The observed absorption changes in the spectrum at 468 nm were fit to eq 5 (inset). (B) The titration of PpRen (10 μM) with sulfite (0−310 mM). The observed absorption changes in the spectrum at 452 nm were fit to eq 5 (inset).

equation, a dissociation constant for sulfite of 105 mM was obtained, substantially weaker than the sulfite affinity observed for HsRen (K_{SO_3} = 1.8 mM).

Structure of the PpRen·β-NAD$^+$ and PpRen·β-NADH Complexes. PpRen proved to be highly apt to form crystals. Both rectangular rods and hexagonal plates were obtained using the conditions that were provided with the PDB ID 3KKJ structure deposited by the NESGC. Only the plate-like crystals diffracted. Structures of the PpRen·β-NAD$^+$ (1.78 Å) and the PpRen·β-NADH (2.0 Å) complexes were obtained by soaking (Table 1). Respectively, these structures are the PpRen$_{ox}$· product (EP) complex and a close representation of the PpRen· substrate (ES) complex. For both structures, two protomers of PpRen are arranged together with a large primarily van der Waals contact interface of ∼1100 Å^2 in which no ionic pairs and only eight hydrogen bonds contribute to the association of the protomers.

Despite low sequence identity (19%), the fold of PpRen is highly similar to that of HsRen (PDB ID 3QJ4), with an RMSD of 2.1 Å for 298/326 Cα atoms (Figure 5). It is interesting to note that the initial structure of PpRen deposited in the PDB (ID 3KKJ) was the search model used to solve the structure of HsRen by molecular replacement. This study therefore serves as the functional assignment of the 3KKJ protein, annotated previously as an amine oxidase. The renalase fold is observed with numerous redox-active flavoproteins.[42] However, the constellation of conserved active site residues is unique to renalase activity (Figure 6). Consistent with the observations of Milani et al.[42] (that pertain to renalase sequences from Animalia), the active site opening is lined with three aromatic residues. In two of the three positions, only the aromatic character of the side chain is conserved (PpRen W212, F204 corresponding to F223, Y214 in HsRen), whereas the third is a conserved tyrosine (PpRen Y57 corresponding to Y62 in HsRen). The inner surfaces of the active site pack closely to the *si* face of the flavin isoalloxazine and provide a substrate binding cavity adjacent to the *re* face. Conserved residues that line the substrate-binding cavity are H232 (HsRen H245) and W276 (HsRen W288). A guanidino group is supplied by R280 (HsRen Q292), and a similar placement of a guanidino group is accomplished in HsRen from R193 (PpRen T185) that is

DOI: 10.1021/acs.biochem.5b00451
Biochemistry 2015, 54, 3791−3802

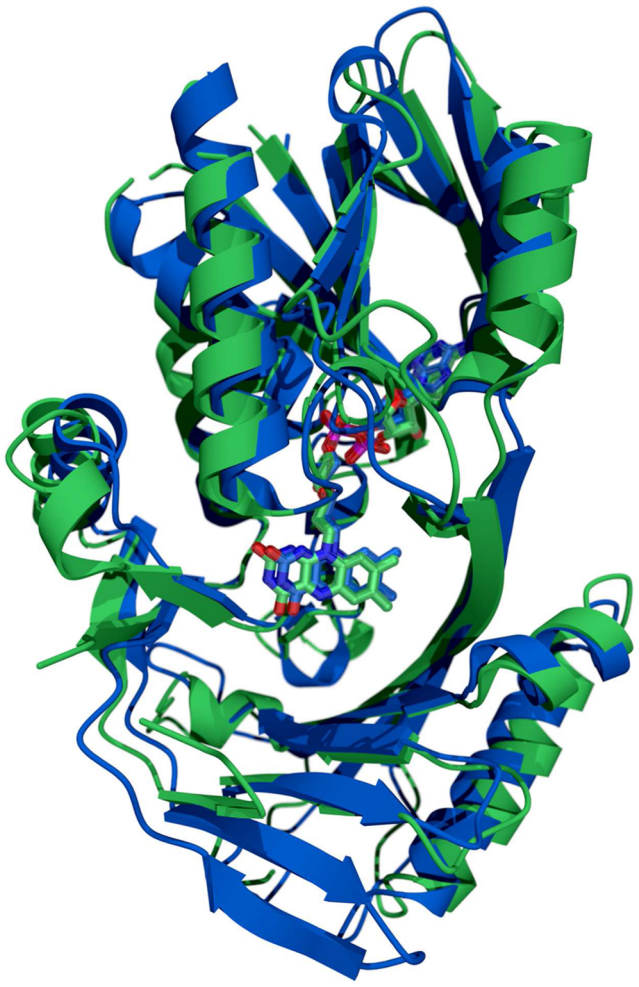

Figure 5. Superposition of the PpRen·β-NADH and HsRen tertiary structures. PpRen·β-NADH is depicted in blue, and HsRen is depicted in green (PDB ID 3QJ4).

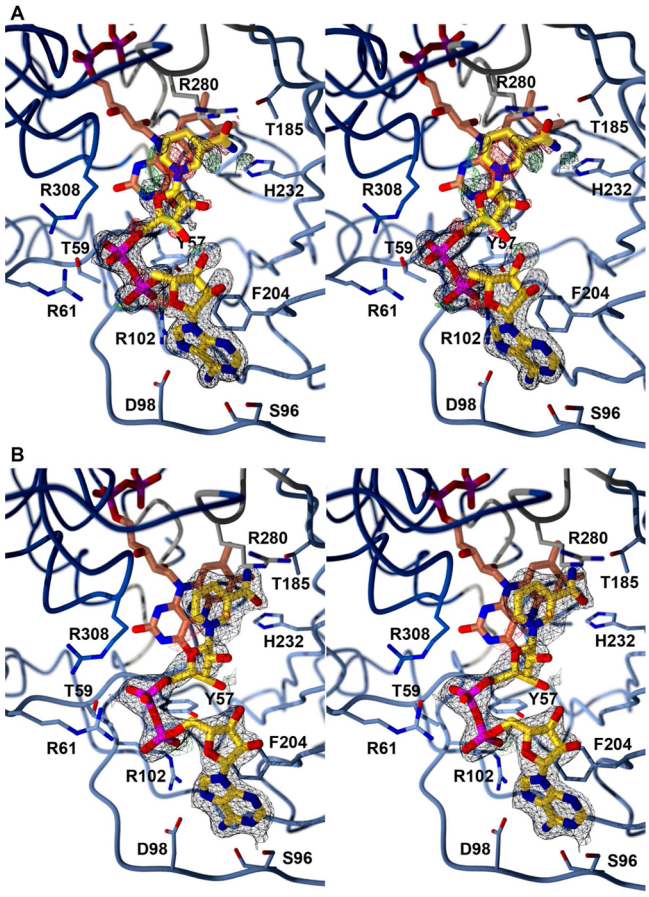

Figure 6. Active site of the PpRen β-NADH and β-NAD$^+$ complexes. (A) Stereoview for the PpRen·β-NAD$^+$ complex showing the $2|F_o| - |F_c|$ simulated annealing composite omit electron density of the ligand (black) contoured at 1.0σ and $|F_o| - |F_c|$ electron density contoured at 3.0σ (green) and −3.0σ (red). (B) Stereoview for the PpRen·β-NADH complex showing the $2|F_o| - |F_c|$ simulated annealing composite omit electron density of the ligand (black) contoured at 1.0σ and $|F_o| - |F_c|$ electron density contoured at 3.0σ (green) and −3.0σ (red).

conserved in Animalia and extends from a different element of the secondary structure.

The primary advancement in understanding the chemistry of renalase was that the PpRen structures were solved with catalytically relevant ligands occupying the active site cavity. Stereoviews of the active site with both ligands and representative ligand density are depicted in Figure 6. The PpRen·β-NADH complex structure provides a representation of the ES complex. The reduced nicotinamide base of β-NADH has an overall neutral charge and is ostensibly isosteric with the bases of 2DHNAD(P) or 6DHNAD(P) and presumably localizes in a position similar to that of the native substrates. Evidence of this is that the 2 position of the base is most proximal to the N5 of the isoalloxazine (3.6 Å), the assumed position of hydride delivery, in an analogous position to that observed in other NAD(P)H/isoalloxazine complexes[60,61] (Figure 7B,C). No evidence for partial occupancy of a 6 position reduction conformer is observed, suggestive of the apparent preference for 2DHNAD(P) isomers that were observed to reduce the enzyme ∼500-fold more rapidly than 6DHNAD(P) isomers (Figure 2 and Table 2). One possible explanation for this apparent conformer bias is that threonine 185 (that occupies the position of a conserved arginine in animal renalases, see below) donates an apparent hydrogen bond to the nicotinamide amide oxygen, stabilizing the pose that promotes donation of the hydride from the 2 position (Figures 6 and 7). Manually flipping the nicotinamide base in the PpRen·β-NADH model followed by additional refinement did not substantially alter the electron density for the pyridyl ring (data not shown). In this alternate pose, a potential interaction is observed from the dihydronicotinamide amido nitrogen to the backbone carbonyl of G307. The PpRen·β-NAD$^+$ structure is that of the product complex. Despite a 1.78 Å resolution, the electron density map for this complex indicated very low occupancy of the base and the ribose that form the nicotinamide nucleoside. It is suggested that the proximity of the R280 (R193 in HsRen) guanidino group plays an important role in ejecting the positively charged nicotinamide product (β-NAD(P)$^+$) from the active site. We observe that the guanidino group is displaced in the PpRen·β-NAD$^+$ structure from the position that it occupies in the PpRen·β-NADH complex structure by 2.6 Å, consistent with charge repulsion.

The ADP moiety of both ligands is anchored in the same position on the surface of the protein (Figure 7). In this binding pose, the two ribose units emerge from the pyrophosphate moiety approximately parallel to one another, a position that places the respective 3′-hydroxyl groups within

DOI: 10.1021/acs.biochem.5b00451
Biochemistry 2015, 54, 3791−3802

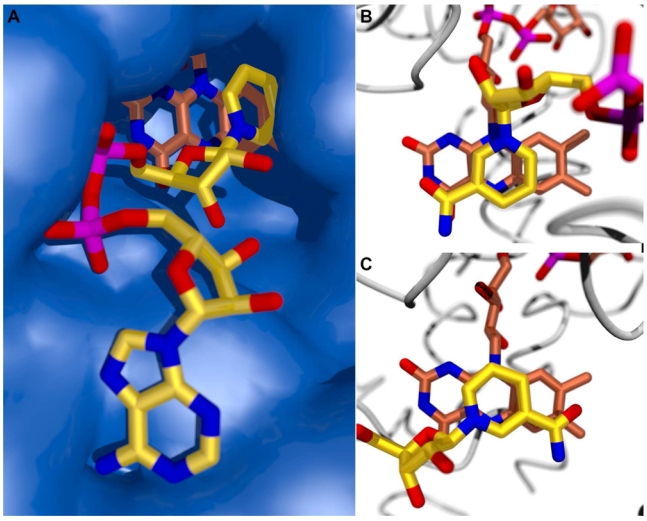

Figure 7. Reductive pose of nicotinamide dinucleotide substrates. (A) The relative positions of β-NADH and FAD on the solvent-accessible surface of PpRen. (B) The reductive complex of glutathione reductase in complex with β-NADH (PDB ID 1GRB) depicting the position of the nicotinamide 4-position 3.4 Å from the flavin isoalloxazine N5. (C) The reductive complex of PpRen in complex with β-NADH (PDB ID 4ZCC) depicting the position of the nicotinamide 2-position 3.6 Å from the flavin isoalloxazine N5.

2.9 Å. Although uncommon, this conformation does not provide an obvious explanation for the observed substrate binding preference of PpRen, where β-NAD$^+$-derived substrates bind ~50-fold more tightly than those derived from β-NADP$^+$.

DISCUSSION

The current consensus understanding for the function of renalase is that it is an animal enzyme/hormone whose catalytic activity lowers blood pressure and modulates the contraction rate of the heart by oxidative consumption of catecholamine substrates (critical evaluations of this claimed catalytic role are available[62−64]). This entrenched perception of the catalytic function of this enzyme has persisted in the literature since the progenitor article claimed to simultaneously discover the enzyme, its catalytic activity, and its physiological role.[1] We, and others, have disputed this claim and have offered evidence and counter arguments that undermine the link to catecholamines.[10−12,39,50,51,65] Moreover, the recent discovery by our group that renalase has genuine catalytic behavior with two β-NAD(P)H isomers[39] casts further doubt over the claim of extracellular catecholamine oxidase activity. This new activity for renalase is more consistent with an intracellular housekeeping metabolic function. In this role, β-NAD(P)H isomers, which we presume to arise in nonspecific reduction events are recycled back to the nicotinamide dinucleotide pool by oxidation (forming β-NAD(P)$^+$) to prevent inhibition of dehydrogenase enzymes. Such an activity would be expected to be generally advantageous to living organisms and therefore likely to be detectable in kingdoms outside Animalia. In this article, we present the first account of a bacterial form of

Scheme 3. Catalytic Cycle of PpRen with 2DHNAD as a Substrate

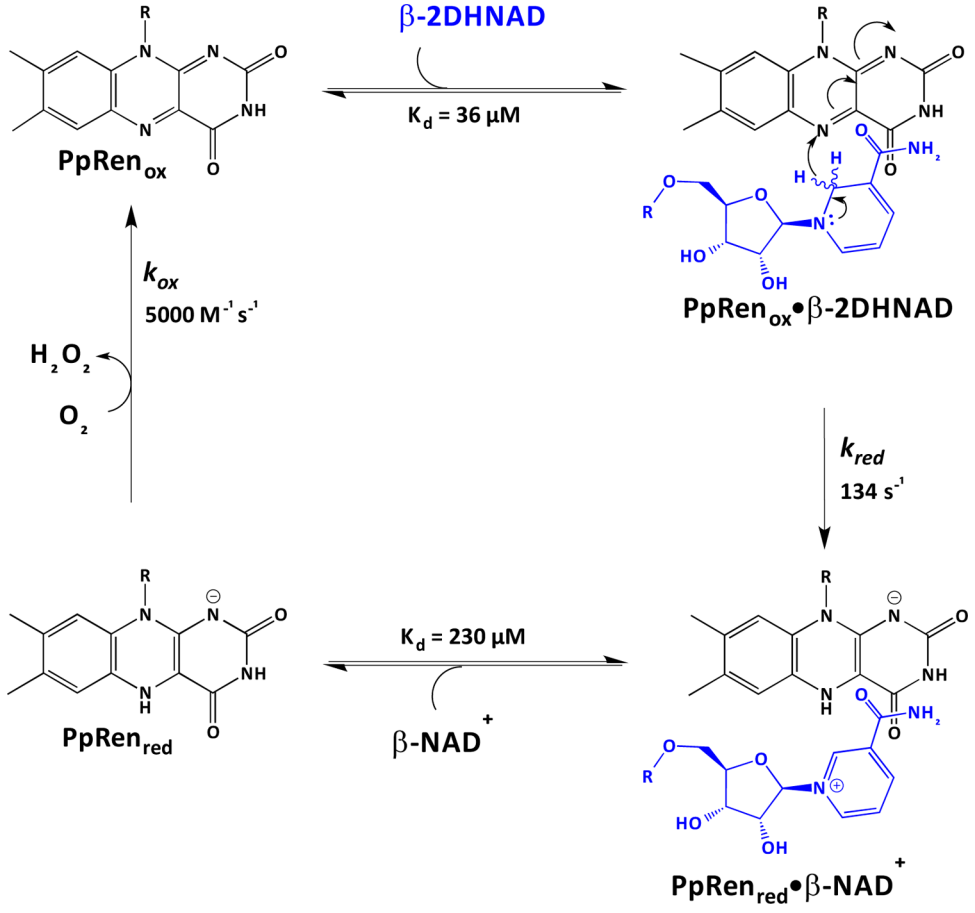

DOI: 10.1021/acs.biochem.5b00451
Biochemistry 2015, 54, 3791−3802

renalase. In addition to the substrate profile, kinetics of catalysis, and substrate/ligand preferences, we also show the structures of the enzyme in complexes with catalytically relevant NAD ligands that have poses consistent with this newly identified activity.

PpRen was first identified in 2009 by the NESGC, and in the absence of known function, it was given a generic, amine oxidase designation (PDB ID 3KKJ). In 2011, the Aliverti group solved the structure of HsRen using 3KKJ as a search model in a molecular replacement strategy (PDB ID 3Qj4).[42] The striking similarity of the apparent active sites of HsRen and 3KKJ led us to conclude that the 3KKJ structure was from a bacterial form of renalase. The data obtained with this enzyme support that it has the same function as that of HsRen. In the presence of a mixture of 2DHNAD(P), 4DHNAD(P) (β-NAD(P)H), and 6DHNAD(P), PpRen oxidizes only the 2- and 6-dihydro isomers, as was observed for the human enzyme (Figure 1). Both β-NAD^+- and β-$NADP^+$-derived substrates induce relative rapid reduction of the PpRen flavin isoalloxazine ring and induce multiple turnovers, indicating that they are genuine substrates for PpRen (Figure 2).

We have proposed that the true function of renalase is to scavenge NAD(P)H isomers to alleviate inhibition of primary metabolism. Solely in terms of dissociation constant, the substrate preference of PpRen would appear to be for β-NAD^+-derived substrates. Both 2DHNAD and 6DHNAD bind 10−50-fold more tightly than do 2DHNADP and 6DHNADP (Figure 2). However, substrate preference (or scavenging efficiency) is a function of both dissociation constant and the rate constant for the largely irreversible hydride transfer to the flavin, and the 6-dihydro substrates reduce PpRen considerably more slowly than the 2-dihydro substrates. When the relative rate constants for reduction and dissociation constants are compared as a ratio (k_{red}/K_d), PpRen has a 300−500−fold preference for 2-DHNAD(P) substrates. It is conceivable that this substrate preference mirrors a 2DHNAD(P) inhibitory susceptibility of one or more of the primary metabolism dehydrogenases in *P. phaseolicola*. The structures of PpRen·β-NADH and PpRen·β-NAD^+ do not reveal the basis of β-NAD^+-derived isomer binding selectivity (Figures 3 and 4A). In both the PpRen·β-NADH and PpRen·β-NAD^+ structures, the oxygen atom of the 2′-hydroxyl of the adenine nucleotide riboside has no interacting residue or steric constraint within an 8 Å sphere (Figure 7A).

It would appear that renalase's primary catalytic purpose is to accept the hydride, as reoxidation of the enzyme occurs with a rate constant only 20-fold greater than that of free $FADH_2$ autoxidation and so is only modestly catalyzed[66,67] (Figure 3). This is unlike most dioxygen-reactive flavoproteins that tend to have reoxidation rate constants at least 2 or 3 orders of magnitude more rapid than that of free flavin.[66,68,69] There is no spectrophotometric evidence for the dissociation of the β-$NAD(P)^+$ product in the reductive half-reaction, but its egress is assumed to be rapid compared to the rate constant for reoxidation at atmospheric levels of dioxygen ($\sim$1 s^{-1}) (Figures 3 and 6). Scheme 3 provides a summary of the kinetic and chemical mechanism conclusions for PpRen in turnover with the preferred substrate, 2DHNAD, that were made from our observations. In this scheme, the substrates bind rapidly and transfers a hydride to the flavin isoalloxazine N5. The release of products has an obligate order in which β-$NAD(P)^+$ dissociates before dioxygen reacts with the reduced flavin. This ordered release of products is based on the observation that exogenous β-NAD^+ can completely suppress the reoxidation of the enzyme. Once β-NAD(P)+ has dissociated, the flavin reoxidizes with a rate constant that would be the *in vitro* rate-limiting process under conditions of atmospheric dioxygen.

The PpRen structures represent a significant advancement in our understanding of the catalysis of this enzyme. Together, the PpRen·β-NADH and PpRen·β-NAD^+ structures offer evidence of the nature of the ES and EP complexes, respectively. The reduction reaction catalyzed by renalase is exceedingly simple: the transfer of a hydride equivalent to the isoalloxazine of a flavin. The primary difference between this and numerous other enzymes is that the substrate nicotinamide is bound to afford hydride transfer from alternate positions of the pyridyl base (Figure 7). Possibly the most interesting aspect of renalase chemistry is that it accommodates reduction from both the 2 and 6 positions and therefore must have binding modes for both substrate types. The structure of PpRen with β-NADH bound has the nicotinamide positioned such that the 2 position of the base is 3.6 Å from and directly over the N5 of the isoalloxazine ring (Figure 7C). No evidence of a flipped, 6 position reduction conformation, in the form of amide density in the alternate meta-position, with respect to the pyridyl nitrogen, is observed. Moreover, no density indicative of a lateral displacement of the nicotinamide to place the 6 position proximal to the flavin N5 is observed. As such, it would appear that the rapid reduction rate constants observed with 2DHNAD(P) substrates are due to a more naturally optimized position whose conformer was selected in the crystalline state by the hydrogen-bonding interaction with threonine 185.

Consistent with the relatively simple reaction being catalyzed, the number of conserved active site residues in renalase is small. The inner surface of the flavin reface substrate cavity has only three fully conserved residues: H232, R280, and W276. Formally, R280 is not positionally conserved, as it extends from a different secondary structural element in the bacterial enzyme (R193 in HsRen). However, the guanidino group of both residues resides in similar positions in the active site. It is posited that this charged residue is responsible for expulsion of the oxidized nicotinamide after hydride transfer and potentially facilitates the reduction chemistry by promoting the formation of the dihydroflavin anion. H232 is conserved in all known or annotated forms of renalase (H245 in HsRen). This residue is not required for acid/base chemistry in the reductive half-reaction but may serve to add to the positive potential toward the internal reaches of the active site. H232 may participate in acid/base chemistry in the oxidative half reaction by shuttling protons to aid rapid elimination of hydrogen peroxide from a transient C4a-(hydro)peroxyflavin during the oxidative half-reaction. This histidine is positioned 5.0 Å from the flavin N5 and C4a positions with both the β-NADH and β-NAD^+ ligands bound.

This study identifies the first known bacterial form of renalase. Defining true catalytic substrates for the human enzyme has both prompted re-evaluation of the true function of this enzyme and provided a means to definitively identify this activity in other organisms, including those without circulatory systems. With regard to the catalytic role of renalase, it has become very clear that claims concerning activity with catecholamines were quite incorrect and were based on the propensity of such molecules to autoxidize in the presence of dioxygen. The elaboration of these claims throughout the past decade warrants some retrospection. While the observations included here and in prior work do not rule out a noncatalytic

DOI: 10.1021/acs.biochem.5b00451
Biochemistry 2015, 54, 3791−3802

moonlighting influence on vascular tone, they do argue strongly that the catalytic role of renalase serves an intracellular function that eliminates an inhibition of primary metabolism by β-NAD(P)H isomers.

AUTHOR INFORMATION

Corresponding Author

*Phone: (414) 940 0059. Fax: (414) 229 5530. E-mail: moran@uwm.edu.

Funding

This research was supported National Science Foundation grants to G.R.M (CHE-1402475) and N.R.S. (MCB-1157392) and by a UWM Research Growth Initiative Grant to G.R.M.

Notes

The authors declare no competing financial interest.

ABBREVIATIONS

PpRen, renalase from *Pseudomonas syringae* (van Hall pathovar *phaseolicola* strain 1448A); HsRen, renalase from *Homo sapien*; PDB, Protein Data Bank; NESGC, North East Structural Genomics Consortium; HPLC, high-performance liquid chromatography; FAD, flavin adenine dinucleotide; β-NADPH, reduced nicotinamide adenine dinucleotide phosphate; β-NADH (4DHNAD), reduced nicotinamide adenine dinucleotide; β-NAD^+, oxidized nicotinamide adenine dinucleotide; 2DHNAD, 2-dihydronicotinamide adenine dinucleotide; 6DHNAD, 6-dihydronicotinamide adenine dinucleotide; IPTG, isopropyl-β-D-thioglactopyranoside; HEPES, 2-[4-(2-hydroxyethyl)piperazin-1-yl]ethanesulfonic acid; LB, Luria–Bertani; PCR, polymerase chain reaction

REFERENCES

(1) Xu, J., Li, G., Wang, P., Velazquez, H., Yao, X., Li, Y., Wu, Y., Peixoto, A., Crowley, S., and Desir, G. V. (2005) Renalase is a novel, soluble monoamine oxidase that regulates cardiac function and blood pressure. *J. Clin. Invest. 115*, 1275–1280.

(2) Desir, G. V. (2007) Renalase is a novel renal hormone that regulates cardiovascular function. *J. Am. Soc. Hypertens. 1*, 99–103.

(3) Xu, J., and Desir, G. V. (2007) Renalase, a new renal hormone: its role in health and disease. *Curr. Opin. Nephrol. Hypertens. 16*, 373–378.

(4) Zhao, Q., Fan, Z., He, J., Chen, S., Li, H., Zhang, P., Wang, L., Hu, D., Huang, J., Qiang, B., and Gu, D. (2007) Renalase gene is a novel susceptibility gene for essential hypertension: a two-stage association study in northern Han Chinese population. *J. Mol. Med. 85*, 877–885.

(5) Desir, G. V. (2008) Renalase deficiency in chronic kidney disease, and its contribution to hypertension and cardiovascular disease. *Curr. Opin. Nephrol. Hypertens. 17*, 181–185.

(6) Desir, G. V. (2009) Regulation of blood pressure and cardiovascular function by renalase. *Kidney Int. 76*, 366–370.

(7) Farzaneh-Far, R., Desir, G. V., Na, B., Schiller, N. B., and Whooley, M. A. (2010) A functional polymorphism in renalase (Glu37Asp) is associated with cardiac hypertrophy, dysfunction, and ischemia: data from the heart and soul study. *PLoS One 5*, e13496.

(8) Li, G., Xu, J., Wang, P., Velazquez, H., Li, Y., Wu, Y., and Desir, G. V. (2008) Catecholamines regulate the activity, secretion, and synthesis of renalase. *Circulation 117*, 1277–1282.

(9) Desir, G. V., Tang, L., Wang, P., Li, G., Sampaio-Maia, B., Quelhas-Santos, J., Pestana, M., and Velazquez, H. (2012) Renalase lowers ambulatory blood pressure by metabolizing circulating adrenaline. *J. Am. Heart Assoc. 1*, e002634.

(10) Boomsma, F., and Tipton, K. F. (2007) Renalase, a catecholamine-metabolising enzyme? *J. Neural Transm. 114*, 775–776.

(11) Eikelis, N., Hennebry, S. C., Lambert, G. W., and Schlaich, M. P. (2011) Does renalase degrade catecholamines? *Kidney Int. 79*, 1380. Author reply, 1380–1381.

(12) Pandini, V., Ciriello, F., Tedeschi, G., Rossoni, G., Zanetti, G., and Aliverti, A. (2010) Synthesis of human renalase1 in *Escherichia coli* and its purification as a FAD-containing holoprotein. *Protein Expression Purif. 72*, 244–253.

(13) Medvedev, A. E., Veselovsky, A. V., and Fedchenko, V. I. (2010) Renalase, a new secretory enzyme responsible for selective degradation of catecholamines: achievements and unsolved problems. *Biochemistry 75*, 951–958.

(14) Buraczynska, M., Zukowski, P., Buraczynska, K., Mozul, S., and Ksiazek, A. (2011) Renalase gene polymorphisms in patients with type 2 diabetes, hypertension and stroke. *NeuroMol. Med. 13*, 321–327.

(15) Desir, G. V. (2011) Role of renalase in the regulation of blood pressure and the renal dopamine system. *Curr. Opin. Nephrol. Hypertens. 20*, 31–36.

(16) Gu, R., Lu, W., Xie, J., Bai, J., and Xu, B. (2011) Renalase deficiency in heart failure model of rats—a potential mechanism underlying circulating norepinephrine accumulation. *PLoS One 6*, e14633.

(17) Przybylowski, P., Malyszko, J., Kozlowska, S., Koc-Zorawska, E., and Mysliwiec, M. (2011) Serum renalase depends on kidney function but not on blood pressure in heart transplant recipients. *Transplant. Proc. 43*, 3888–3891.

(18) Wu, Y., Xu, J., Velazquez, H., Wang, P., Li, G., Liu, D., Sampaio-Maia, B., Quelhas-Santos, J., Russell, K., Russell, R., Flavell, R. A., Pestana, M., Giordano, F., and Desir, G. V. (2011) Renalase deficiency aggravates ischemic myocardial damage. *Kidney Int. 79*, 853–860.

(19) Baraka, A., and El Ghotny, S. (2012) Cardioprotective effect of renalase in 5/6 nephrectomized rats. *J. Cardiovasc. Pharmacol. Ther. 17*, 412–416.

(20) Desir, G. (2012) Novel insights into the physiology of renalase and its role in hypertension and heart disease. *Pediatr. Nephrol. 27*, 719–725.

(21) Desir, G. V., Wang, L., and Peixoto, A. J. (2012) Human renalase: a review of its biology, function, and implications for hypertension. *J. Am. Soc. Hypertens. 6*, 417–426.

(22) Guo, Y., and Jiang, W. (2012) [Research progress with renalase and cardiovascular disease]. *Zhongnan Daxue Xuebao, Yixueban 37*, 537–540.

(23) Zbroch, E., Malyszko, J., Koc-Zorawska, E., and Mysliwiec, M. (2012) Renalase, kidney function, and markers of endothelial dysfunction in renal transplant recipients. *Pol. Arch. Med. Wewn. 122*, 40–44.

(24) Zbroch, E., Malyszko, J., Malyszko, J. S., Koc-Zorawska, E., and Mysliwiec, M. (2012) Renalase, a novel enzyme involved in blood pressure regulation, is related to kidney function but not to blood pressure in hemodialysis patients. *Kidney Blood Pressure Res. 35*, 395–399.

(25) Czarkowska-Paczek, B., Zendzian-Piotrowska, M., Gala, K., Sobol, M., and Paczek, L. (2013) Exercise differentially regulates renalase expression in skeletal muscle and kidney. *Tohoku J. Exp. Med. 231*, 321–329.

(26) Lee, H. T., Kim, J. Y., Kim, M., Wang, P., Tang, L., Baroni, S., D'Agati, V. D., and Desir, G. V. (2013) Renalase protects against ischemic AKI. *J. Am. Soc. Nephrol. 24*, 445–455.

(27) Przybylowski, P., Koc-Zorawska, E., Malyszko, J. S., Mysliwiec, M., and Malyszko, J. (2013) Renalase and endothelial dysfunction in heart transplant recipients. *Transplant. Proc. 45*, 394–396.

(28) Sizova, D., Velazquez, H., Sampaio-Maia, B., Quelhas-Santos, J., Pestana, M., and Desir, G. V. (2013) Renalase regulates renal dopamine and phosphate metabolism. *Am. J. Physiol.: Renal Physiol. 305*, F839–844.

(29) Zbroch, E., Koc-Zorawska, E., Malyszko, J., and Mysliwiec, M. (2013) Circulating levels of renalase, norepinephrine, and dopamine in dialysis patients. *Renal Failure 35*, 673–679.

(30) Desir, G. V., and Peixoto, A. J. (2014) Renalase in hypertension and kidney disease. *Nephrol., Dial., Transplant. 29*, 22–28.

DOI: 10.1021/acs.biochem.5b00451
Biochemistry 2015, 54, 3791–3802

(31) Li, X., Huang, R., Xie, Z., Lin, M., Liang, Z., Yang, Y., and Jiang, W. (2014) Renalase, a new secretory enzyme: its role in hypertensive−ischemic cardiovascular diseases. *Med. Sci. Monit. 20*, 688−692.
(32) Sonawane, P. J., Gupta, V., Sasi, B. K., Kalyani, A., Natarajan, B., Khan, A. A., Sahu, B. S., and Mahapatra, N. R. (2014) Transcriptional regulation of the novel monoamine oxidase renalase: crucial roles of transcription factors Sp1, STAT3, and ZBP89. *Biochemistry 53*, 6878−6892.
(33) Wang, F., Cai, H., Zhao, Q., Xing, T., Li, J., and Wang, N. (2014) Epinephrine evokes renalase secretion via alpha-adrenoceptor/NF-kappaB pathways in renal proximal tubular epithelial cells. *Kidney Blood Pressure Res. 39*, 252−259.
(34) Wang, F., Huang, B., Li, J., Liu, L., and Wang, N. (2014) Renalase might be associated with hypertension and insulin resistance in Type 2 diabetes. *Renal Failure 36*, 552−556.
(35) Wang, F., Li, J., Xing, T., Xie, Y., and Wang, N. (2015) Serum renalase is related to catecholamine levels and renal function. *Clin. Exp. Nephrol. 19*, 92−98.
(36) Wang, Y., Liu, F. Q., Wang, D., Mu, J. J., Ren, K. Y., Guo, T. S., Chu, C., Wang, L., Geng, L. K., and Yuan, Z. Y. (2014) Effect of salt intake and potassium supplementation on serum renalase levels in Chinese adults: a randomized trial. *Medicine 93*, e44.
(37) Wybraniec, M. T., Mizia-Stec, K., Trojnarska, O., Chudek, J., Czerwienska, B., Wikarek, M., and Wiecek, A. (2014) Low plasma renalase concentration in hypertensive patients after surgical repair of coarctation of aorta. *J. Am. Soc. Hypertens. 8*, 464−474.
(38) Quelhas-Santos, J., and Pestana, M. (2015) Plasma renalase expression in chronic kidney disease: differences and similarities between humans and rats. *Curr. Hypertens. Rev. 10*, 166−170.
(39) Beaupre, B. A., Hoag, M. R., Roman, J., Forsterling, F. H., and Moran, G. R. (2015) Metabolic function for human renalase: oxidation of isomeric forms of beta-NAD(P)H that are inhibitory to primary metabolism. *Biochemistry 54*, 795−806.
(40) Lowry, O. H., Passonneau, J. V., and Rock, M. K. (1961) The stability of pyridine nucleotides. *J. Biol. Chem. 236*, 2756−2759.
(41) Dalziel, K. (1963) The purification of nicotinamide adenine dinucleotide and kinetic effects of nucleotide impurities. *J. Biol. Chem. 238*, 1538−1543.
(42) Milani, M., Ciriello, F., Baroni, S., Pandini, V., Canevari, G., Bolognesi, M., and Aliverti, A. (2011) FAD-binding site and NADP reactivity in human renalase: a new enzyme involved in blood pressure regulation. *J. Mol. Biol. 411*, 463−473.
(43) Schreuder, H. A., Prick, P. A., Wierenga, R. K., Vriend, G., Wilson, K. S., Hol, W. G., and Drenth, J. (1989) Crystal structure of the *p*-hydroxybenzoate hydroxylase-substrate complex refined at 1.9 Å resolution. Analysis of the enzyme-substrate and enzyme-product complexes. *J. Mol. Biol. 208*, 679−696.
(44) Birchfield, N. B., Latli, B., and Casida, J. E. (1998) Human protoporphyrinogen oxidase: relation between the herbicide binding site and the flavin cofactor. *Biochemistry 37*, 6905−6910.
(45) Mizutani, H., Miyahara, I., Hirotsu, K., Nishina, Y., Shiga, K., Setoyama, C., and Miura, R. (1996) Three-dimensional structure of porcine kidney D-amino acid oxidase at 3.0 Å resolution. *J. Biochem. 120*, 14−17.
(46) Faust, A., Niefind, K., Hummel, W., and Schomburg, D. (2007) The structure of a bacterial L-amino acid oxidase from *Rhodococcus opacus* gives new evidence for the hydride mechanism for dehydrogenation. *J. Mol. Biol. 367*, 234−248.
(47) Pawelek, P. D., Cheah, J., Coulombe, R., Macheroux, P., Ghisla, S., and Vrielink, A. (2000) The structure of L-amino acid oxidase reveals the substrate trajectory into an enantiomerically conserved active site. *EMBO J. 19*, 4204−4215.
(48) Chen, Y., Yang, Y., Wang, F., Wan, K., Yamane, K., Zhang, Y., and Lei, M. (2006) Crystal structure of human histone lysine-specific demethylase 1 (LSD1). *Proc. Natl. Acad. Sci. U.S.A. 103*, 13956−13961.
(49) Klemm, A., Steiner, T., Flotgen, U., Cumme, G. A., and Horn, A. (1997) Determination, purification, and characterization of alpha-NADH and alpha-NADPH. *Methods Enzymol. 280*, 171−186.
(50) Beaupre, B. A., Carmichael, B. R., Hoag, M. R., Shah, D. D., and Moran, G. R. (2013) Renalase is an alpha-NAD(P)H oxidase/anomerase. *J. Am. Chem. Soc. 135*, 13980−13987.
(51) Beaupre, B. A., Hoag, M. R., Carmichael, B. R., and Moran, G. R. (2013) Kinetics and equilibria of the reductive and oxidative half-reactions of human renalase with alpha-NADPH. *Biochemistry 52*, 8929−8937.
(52) Strickland, S., Palmer, G., and Massey, V. (1975) Determination of dissociation constants and specific rate constants of enzyme−substrate (or protein−ligand) interactions from rapid reaction kinetic data. *J. Biol. Chem. 250*, 4048−4052.
(53) Otwinowski, Z., and Minor, W. (1997) Processing of X-ray diffraction data collection in oscillation mode. *Methods Enzymol. 276*, 307−325.
(54) McCoy, A. J., Grosse-Kunstleve, R. W., Adams, P. D., Winn, M. D., Storoni, L. C., and Read, R. J. (2007) Phaser crystallographic software. *J. Appl. Crystallogr. 40*, 658−674.
(55) Emsley, P., Lohkamp, B., Scott, W. G., and Cowtan, K. (2010) Features and development of Coot. *Acta Crystallogr., Sect. D: Biol. Crystallogr. 66*, 486−501.
(56) Afonine, P. V., Mustyakimov, M., Grosse-Kunstleve, R. W., Moriarty, N. W., Langan, P., and Adams, P. D. (2010) Joint X-ray and neutron refinement with phenix.refine. *Acta Crystallogr., Sect. D: Biol. Crystallogr. 66*, 1153−1163.
(57) Word, J. M., Lovell, S. C., Richardson, J. S., and Richardson, D. C. (1999) Asparagine and glutamine: using hydrogen atom contacts in the choice of side-chain amide orientation. *J. Mol. Biol. 285*, 1735−1747.
(58) Urzhumtseva, L., Afonine, P. V., Adams, P. D., and Urzhumtsev, A. (2009) Crystallographic model quality at a glance. *Acta Crystallogr., Sect. D: Biol. Crystallogr. 65*, 297−300.
(59) Chen, V. B., Arendall, W. B., III, Headd, J. J., Keedy, D. A., Immormino, R. M., Kapral, G. J., Murray, L. W., Richardson, J. S., and Richardson, D. C. (2010) MolProbity: all-atom structure validation for macromolecular crystallography. *Acta Crystallogr., Sect. D: Biol. Crystallogr. 66*, 12−21.
(60) Karplus, P. A., and Schulz, G. E. (1987) Refined structure of glutathione reductase at 1.54 Å resolution. *J. Mol. Biol. 195*, 701−729.
(61) Pai, E. F., and Schulz, G. E. (1983) The catalytic mechanism of glutathione reductase as derived from X-ray diffraction analyses of reaction intermediates. *J. Biol. Chem. 258*, 1752−1757.
(62) Malyszko, J., Malyszko, J. S., Rysz, J., Mysliwiec, M., Tesar, V., Levin-Iaina, N., and Banach, M. (2013) Renalase, hypertension, and kidney—the discussion continues. *Angiology 64*, 181−187.
(63) Malyszko, J., Bachorzewska-Gajewska, H., and Dobrzycki, S. (2014) Renalase, kidney and cardiovascular disease: Are they related or just coincidentally associated? *Adv. Med. Sci. 60*, 41−49.
(64) Moran, G. R. (2015) The catalytic function of renalase: a decade of phantoms. *Biochim. Biophys. Acta*, DOI: 10.1016/j.bbapap.2015.04.010.
(65) Baroni, S., Milani, M., Pandini, V., Pavesi, G., Horner, D., and Aliverti, A. (2013) Is renalase a novel player in catecholaminergic signaling? The mystery of the catalytic activity of an intriguing new flavoenzyme. *Curr. Pharm. Des. 19*, 2540−2551.
(66) Gadda, G. (2012) Oxygen activation in flavoprotein oxidases: the importance of being positive. *Biochemistry 51*, 2662−2669.
(67) Valton, J., Mathevon, C., Fontecave, M., Niviere, V., and Ballou, D. P. (2008) Mechanism and regulation of the two-component FMN-dependent monooxygenase ActVA-ActVB from *Streptomyces coelicolor*. *J. Biol. Chem. 283*, 10287−10296.
(68) Entsch, B., Massey, V., and Ballou, D. P. (1974) Intermediates in flavoprotein catalyzed hydroxylations. *Biochem. Biophys. Res. Commun. 57*, 1018−1025.
(69) Crozier-Reabe, K., and Moran, G. R. (2012) Form follows function: structural and catalytic variation in the class a flavoprotein monooxygenases. *Int. J. Mol. Sci. 13*, 15601−15639.

DOI: 10.1021/acs.biochem.5b00451
Biochemistry 2015, 54, 3791−3802